



Responses of surface modeling and optimization of Brilliant Green adsorption by adsorbent prepared from *Citrus limetta* peel

Prasad Sudamalla^a, Saravanan Pichiah^b, Matheswaran Manickam^{a,*}

^aDepartment of Chemical Engineering, National Institute of Technology, Tiruchirappalli 620 015, India
Tel. +91 4312503120; Fax: +91 4312503102; email: matheswaran@nitt.edu.in

^bDepartment of Civil & Environmental Engineering, University of Malaya, Kuala Lumpur 50603, Malaysia

Received 9 January 2012; Accepted 29 April 2012

ABSTRACT

An adsorbent prepared from *Citrus limetta* peel was used to study its sorption potential on removing Brilliant Green dye. The initial dye concentration and sorbent dosages were varied between 10–100 mg/L and 0.5–5.0 g/L, respectively. The influence of parameters like pH, temperature, initial concentration, and adsorbent dosage on dye adsorption was also studied. A maximum dye removal of 95% was achieved with an initial concentration of 10 mg/L. The percentage removal was mathematically described as a function of experimental parameters and modeled through response surface methodology. The results show that the responses on adsorption of dyes were significantly affected by the synergistic effect of linear term of time and dosage and the quadratic term of temperature and time. A 2⁴ full factorial design of experiments was adopted and statistical analysis was performed in the form of ANOVA and student “t” test, which gave good interpretation in terms of interaction of experimental parameters.

Keywords: Adsorption; ANOVA; Brilliant Green dye; *Citrus limetta* peel; Response surface methodology; Student’s t-test

1. Introduction

Dyes are one of the major constituents of wastewater, discharged by many industries including textile processing, cosmetics, printing, dyeing, food coloring, pulp, and paper mill. Their presence in water results in allergic dermatitis, skin irritation, cancer, mutations, also prevents sunlight penetration into water, reduces photosynthetic activity, and causes pollution of the environment. Therefore, its removal from the aquatic environment becomes necessary. Several treatment techniques including adsorption, coagulation, flocculation, ozonation, reverse osmosis, chemical oxidation, and biological process are available to remove such

dyes from the industrial effluent [1–4]. Of these techniques, adsorption is one of the cost-effective and user friendly techniques. The adsorption process is an attractive alternative treatment for removal of color if the adsorbent is from bio-waste or naturally available [4].

In recent years, many researchers developed and experimented several low-cost adsorbent materials for dye removal, namely activated carbon (AC), stumpy class coals, peat moss, chitosan and wood, silica gel, natural clay, peat, wood chips, rice husk ash, living or dead microbial biomass, fly ash, shale oil ash, fuller’s earth, Zeolite, Perlite, Alunite, activated slag, and agricultural wastes [5–13]. Among them AC was highly successful due to its high adsorption capacity. However, AC regeneration and reuse is more expensive.

*Corresponding author.

Many attempts have been made to substitute these materials by other equivalents that are biodegradable, low cost, and/or from waste materials [10–14]. This research reports on the potential use of *Citrus limetta* peel as a low-cost adsorbent of Brilliant Green (BG) dye. The adsorption parameters were optimized statistically by adopting 2^4 full factorial designs with response surface methodology (RSM).

The RSM is a designed regression analysis to predict the value of a dependent variable based on the controlled values of the independent variables. It leads to a need for an experimental design which can generate a lot of samples for consumer evaluation in a short duration; making laboratory level tests more efficient. In general, the product optimization time is greatly reduced from traditional “cook and look” optimization techniques. From the parameter estimate, it can be determined which variable contributes most to the prediction model, thereby allowing the product researcher to focus on the variables that are most important to the product acceptance [15,16]. The RSM was used to optimize the experimental parameter for different processes like advanced oxidation process [17–19] and electrochemical oxidation [20] and adsorption [21,22]. The two most commonly practiced designs in RSM are the central composite design (CCD) and the Box–Behnken design [23]. In the present study, CCD with RSM was adopted to optimize the experimental parameters like pH, initial concentration, adsorbent dosage, and temperature for a maximum amount adsorbed and the percentage of removal.

2. Materials and methods

2.1. Chemicals and reagents

The adsorbate, BG dye, C.I. 42040, chemical formula $C_{27}H_{34}N_2O_4S$, MW 482.62; nature basic green was obtained from s.d. Fine Chemicals[®], India. All other reagents used were of analytical grade.

2.2. Preparation and characterization of adsorbent

The *C. limetta* peel was solar dried over a period of time. The dried peel was then crushed in the ball mill and sieved in 60–85 mesh (British Standard Specification) to obtain desired particle size. The material was washed with HCl and distilled water for removing the dissolved matter and dried for 2 h at 120 °C in hot air oven. Thus, the prepared sorbent was utilized for further study.

Particle morphology of the prepared sorbent was examined under scanning electron microscopy (SEM),

samples were dried and coated with gold film in a sputter coater and finally, the morphology was recorded in LEO 1430VP SEM instrument at a magnification of 4,350 at 15 kV. Energy dispersive spectrometer (EDS) analysis was performed to identify the elemental composition of the prepared adsorbent. N_2 adsorption–desorption isotherms were measured with Micromeritics ASAP 2020 Surface Area and Porosity Analyzer V3.00. Prior to analysis, the samples were outgassed at 150 °C for 12 h. The pore-size distribution curves were obtained from the analysis of the desorption portion of the isotherms using the Barrett–Joyner–Halenda (BJH) method and the total pore volume was estimated at a relative pressure of 0.99, assuming full surface saturation with nitrogen. The surface area was calculated using a multipoint Brunauer–Emmett–Teller (BET) model.

2.3. Batch adsorption experiments

All experiments were performed in 250 mL Erlenmeyer flask containing 200 mL of BG solution at concentration ranging from 10 to 100 mg/L and measured quantities of prepared adsorbent (0.5–5 g/L) were added. The samples were agitated at 100 rpm in an orbital shaker maintained at 303, 308, 313, and 318 K, respectively. Based on the preliminary experiments, the equilibrium time was found to be 4 h and the same was adopted in the all other experimental studies. The samples were collected at a regular interval and filtered (Whatman No. 1) and the residual concentration of BG was determined spectrophotometrically using UV–vis spectrophotometer (Jasco USA Model No: V-570) by monitoring absorbance at λ_{max} of 618 nm.

The effect of pH on the percentage removal was investigated over the pH range of 2–11. The pH of the solution was adjusted by addition of 0.1 M HCl or NaOH. The effects of adsorbent dosage (0.5–5 g/L), initial concentration (10–100 mg/L) and temperature (303–318 K) on the adsorption capacity of BG were studied. The percentage removal of dye was calculated using the following relationship:

$$\% \text{ Removal} = \frac{(C_0 - C)}{C_0} \times 100 \quad (1)$$

where C_0 and C (in mg/L) are the initial and at time t of dye concentration, respectively. The adsorption capacity q (mg/g) at equilibrium time was calculated by mass balance relationship Eq. (3) as follows [24]:

$$q = (C_0 - C_e) \times \left(\frac{V}{W}\right) \tag{2}$$

where C_0 and C_e are the initial and equilibrium concentrations (mg/L) of dye in aqueous solution, respectively, V is the volume of the solution (L), and W is the weight of adsorbent (g).

2.4. Response surface methodology

Four independent test variables were chosen for the statistical experimental designs are as follows: temperature (X_1 , K), pH (X_2), adsorbent dosage (X_3 , g/L), and contact time (X_4 , min). The range and the levels of the factors, which varied according to the experimental design, are given in Table 1.

A 2^4 full-factorial experimental design was carried out as a CCD consisting of 31 experiments [25]. The adsorption efficiency depends on process parameters including contact time, adsorbent dosage, pH, and temperature of the solution. In order to study the interaction effects of the factors, experiments were performed with a combination of physical parameters using statistically designed experiments. The coded and the range experiment parameters in the study are given in Table 1. A full second-order polynomial model obtained by multiple regression technique for three factors using the statistical analysis system (SAS) package (SAS Institute, Cary, NC, USA) and MINITAB (Minitab Institute, USA) was adopted to describe the response surface. In developing the regression equation reported by Box and Hunter [26], the test factors were coded according to the following equation:

$$x_i = \frac{X_i - X_{i0}}{\Delta X_i} \tag{3}$$

where x_i is the coded value of the i th independent variable, X_i is the natural value of the i th independent variable, X_{i0} is the natural value of the i th independent variable at the center point, and ΔX_i is the step change value.

Table 1
Range and levels of the experimental variables

Variables	Range and levels				
	-2	-1	0	+1	+2
Temperature, K: (X_1)	25	30	35	40	45
pH: (X_2)	2	4	7	9	11
Adsorbent dosage, g/L: (X_3)	0.5	1.5	2.5	3.5	5
Contact time, min: (X_4)	15	60	150	240	300

$$Y = b_0 + \sum_{i=1}^k b_i x_i + \sum_{i=1}^{k-1} \sum_{j=2}^k b_{ij} x_i x_j + \sum_{i=1}^k b_{ii} x_i^2 + e \tag{4}$$

where Y is the predicted response, b_0 is the offset term, b_i is the linear effect, b_{ii} is the squared effect, and b_{ij} is the interaction effect. The three significant independent variables X_1 , X_2 , and X_3 and the mathematical relationship of the response Y to these variables can be approximated by quadratic/(second degree) polynomial equation as shown below:

$$Y = b_0 + b_1 \cdot X_1 + b_2 \cdot X_2 + b_3 \cdot X_3 + b_4 \cdot X_4 + b_{12} \cdot X_1 X_2 + b_{13} \cdot X_1 X_3 + b_4 \cdot X_1 X_4 + b_{23} \cdot X_2 X_3 + b_{24} \cdot X_2 X_4 + b_{34} \cdot X_3 X_4 + b_{11} \cdot X_1^2 + b_{22} \cdot X_2^2 + b_{33} \cdot X_3^2 + b_{44} \cdot X_4^2 \tag{5}$$

where b_0 is the constant, b_1 , b_2 , and b_3 are the linear coefficients, b_{12} , b_{13} , and b_{23} are the cross product coefficients, and b_{11} , b_{22} , and b_{33} are the quadratic coefficients.

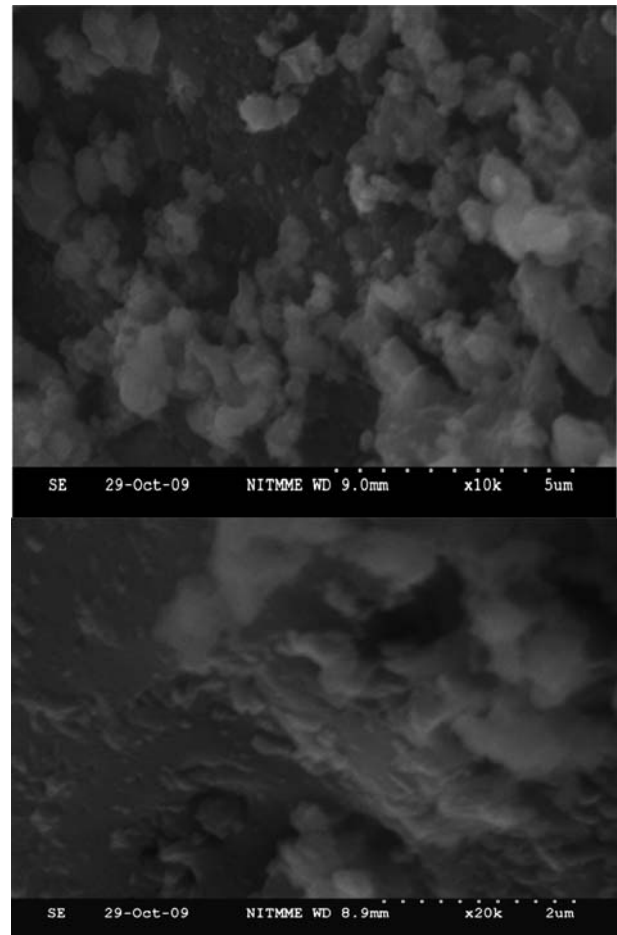


Fig. 1. SEM micrographs of adsorbent prepared from *C. limetta* peel.

3. Results and discussion

3.1. Characterization of adsorbent

SEM is widely used to study the morphological features and surface characteristics of adsorbent materials. The morphology of unburned carbon is shown in Fig. 1. From this figure, it is quite obvious to see that unburned carbon particle had a very porous structure. The carbon particles of different sizes are also observed on the surface or inside the pores. The EDS spectrum of the sample is shown in Fig. 2, where it confirmed the presence of C, Mg, O₂, and Ca. The results presented in Table 2 confirm approximate concentrations, weight percentage, etc. of the elements present in the prepared sample. Carbon predominates over the other elements, which, indicate that the prepared material may have a good adsorption property, thus enabling further experiments to be carried out.

In addition, the BET surface area, micro-mesopore volumes, Density Functional Theory (DFT) pore volume, and average pore width of adsorbent were investigated. Identification of the pore structure of adsorbents, commonly determined by the adsorption of inert gasses [27,28], is an essential procedure prior to liquid sorption. The typical adsorption/desorption

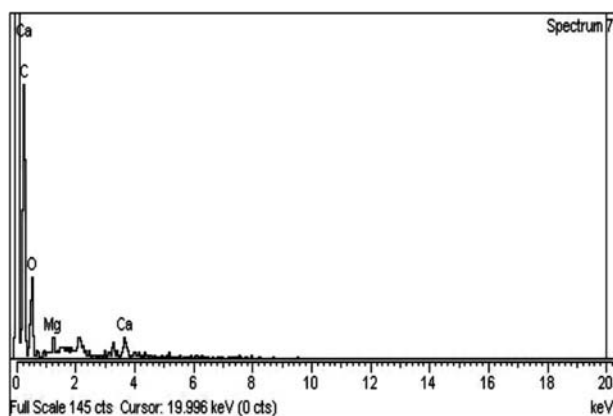


Fig. 2. EDS spectrum of the adsorbent prepared from *C. limetta* peel.

isotherms of N₂ at –196 °C for the ACs prepared from *C. limetta* peel were depicted in Fig. 3(a). The micropore size estimated from the Horvath–Kawazoe method is shown in Fig. 3(b). From the plot, it can be inferred that maximum pore volume is obtained within the radius range of (0–20) Å. It can be observed that at a pore width of 14.568 Å, the gradient of differential pore volume becomes zero, which suggests that the pore volume is maximum at this point. The surface area and total pore volume of the adsorbent prepared from *C. limetta* peel is found to be 85.9 m²/g and 0.254 cm³/g, respectively.

3.2. Effect of contact time

The relationship between the amount of dye adsorbed (%) and contact time (*t*) at different initial dye concentrations is presented in Fig. 4. The rapid uptake of dye was observed at *t*=0 in relation to the equilibrium time irrespective of dye concentration without lag phase. The adsorbent attained equilibrium after approximately 4 h. The percentage removal and amount of dye adsorbed (*q_t*) decreased from 88 to 34% and increased from 3.52 to 13.6 mg/g with an increase in the dye concentrations from 10 to 100 mg/L, respectively. This suggests that for lower initial concentration of dye, the adsorption is very fast. The percentage removal of dye decreases with an increase in initial concentration and takes longer time to reach equilibrium because with an increase in dye concentrations, there will be increased competition for active adsorption sites and the adsorption process will increasingly slow down. This explains the extended adsorption time for higher concentrations. The removal curves are single, smooth, and continuous leading to saturation, suggesting possible monolayer coverage of dye on the surface of adsorbent. The effect of initial dye concentrations on the percentage removal of BG with fixed adsorbent dosage was studied. This figure shows that the percentage removal of BG increases from 34 to 88% with a decrease of initial dye concentrations at adsorbent levels of 3.5 g/L. However, the percentage removal of dye declined

Table 2
EDS analysis of adsorbent prepared from *C. limetta* peel

Element	Approximate concentration	Intensity, corr.	Weight (%)	Weight (%) sigma	Atomic (%)
C, K	114.67	1.3517	84.84	8.15	65.82
O, K	33.07	0.5961	55.46	10.02	32.30
Mg, K	2.05	0.8606	2.38	1.06	0.91
Ca, K	3.94	0.9562	4.12	1.96	0.96

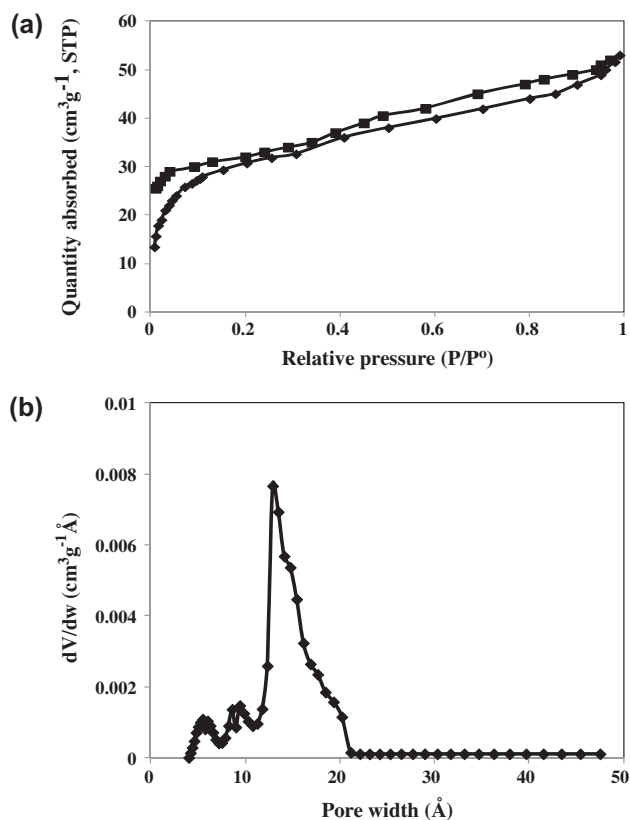


Fig. 3. (a) N₂ adsorption–desorption isotherms and (b) DFT pore size distributions plot of adsorbent prepared from *C. limetta* peel.

with an increase in the initial dye concentration irrespective of adsorbent dosage.

3.3. Effect of pH

The pH of the solution is one of the most important parameter in controlling adsorption. Moreover, it also affects the structural stability of BG dye. This investigation was carried over a pH range of 2–11 with an initial BG concentration of 50 mg/L, adsorbent dosage of 2.5 g/L, and temperature of 303 K. Fig. 5 shows the percentage color removal with a pH change using an unburned carbon adsorbent derived from the *C. limetta* peel. This figure depicts that the a maximum percentage removal of 60% was obtained at pH 4. Beyond that no decline or increment in percentage removal of dye was observed. This is why further experiments were conducted without adjusting the pH. However, it is inferred that the dye is stable at initial solution pH and it becomes unstable if the solution pH is either increased or decreased. BG instability due to the pH change alone may result from structural changes that take place in the BG molecules.

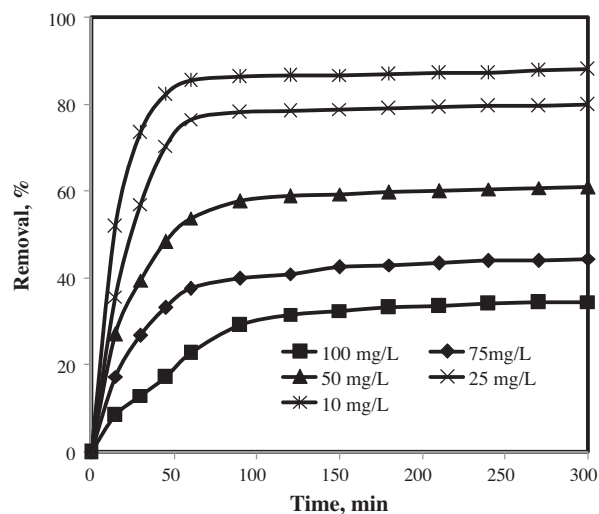


Fig. 4. Effect of contact time on the percentage removal of BG by adsorbent prepared from *C. limetta* peel ($m = 0.5$ g, $T = 303$ K, and medium pH).

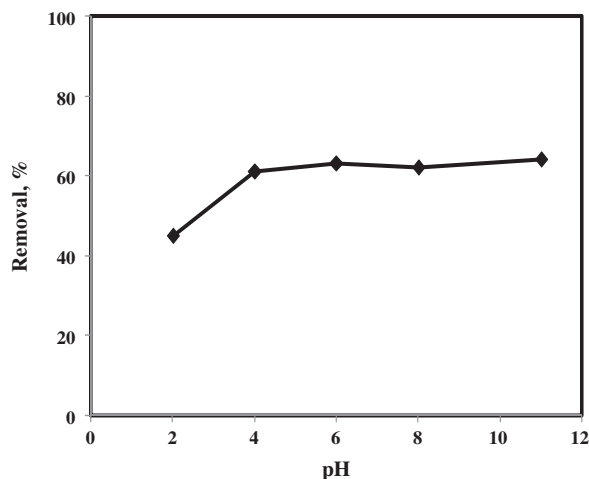


Fig. 5. Effect of pH on the adsorption of BG by adsorbent prepared from *C. limetta* peel ($C_0 = 50$ mg/L, $m = 0.5$ g, $T = 303$ K, and $t = 4$ h).

3.4. Effect of adsorbent dosage

The adsorption capacity of an adsorbent mainly depends on the parameter of adsorbent dosage for a given initial concentration of adsorbate. The effect of adsorbent dosage was studied on the percentage removal of BG at an initial concentration of dye 50 mg/L, temperature 303 K, and pH 4. The percentage removal of dye increases with the increase in dosage of adsorbent (0.5–5 g/L) as observed in Fig. 6. However, at a fixed initial dye concentration of 50 mg/L, the dye uptake decreases from 45.96 mg/g (45.9%) to 6.8 mg/g (68%) with an increase in adsorbent dosage.

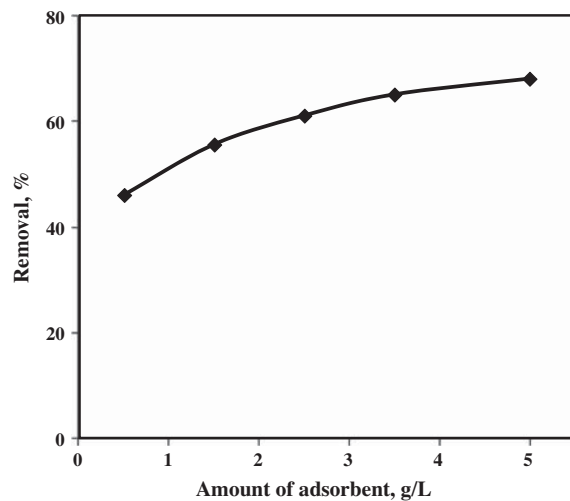


Fig. 6. Effect of adsorbent loading on the sorption of BG by *C. limetta* peel ($C_0=50$ mg/L, $T=303$ K, medium pH, and $t=4$ h).

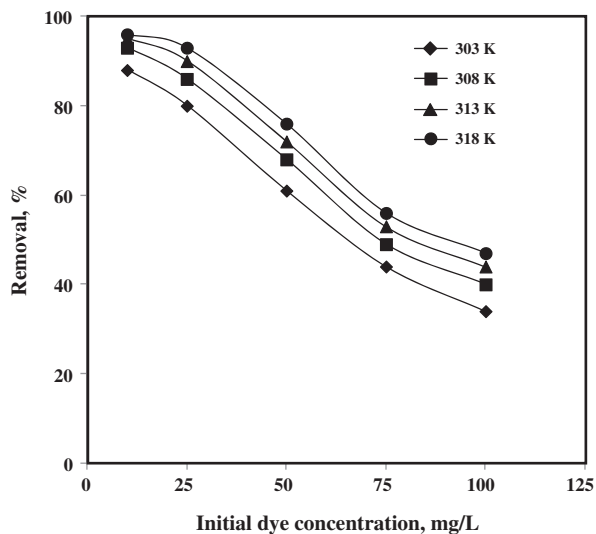


Fig. 7. Effect of temperature on the removal of BG by adsorbent prepared from *C. limetta* peel ($C_0=50$ mg/L, pH=4, and $t=4$ h).

The decrease in the dye uptake value is due to the fragmented effect of flux between adsorbate and adsorbent. The percentage of color removal increases may be due to the increase in adsorbent dosage attributed to the increase in surface area and also the availability of adsorption site.

3.5. Effect of temperature

Fig. 7 shows the plot between percentage removals of BG vs. initial dye concentrations at different

temperatures. The temperature range used in this study varied from 303 to 318 K with the increment of 5 K. Higher temperature increases the rate of adsorption, which resulted in a maximum dye removal of 98% with an initial dye concentration of 10 mg/L. This evidence concludes that an increase in temperature enhances the thermal motion of ions in the solution, thus increasing the adsorption capacity of the adsorbent. Moreover, an increase in temperature simultaneously increases the mass transfer rate of adsorbate molecules across the external boundary layer of adsorbent. This figure shows that with an increase in temperature, the percentage removal of BG increases from 61 to 76% at an initial concentration of 50 mg/L and

Table 3
2⁴ full factorial CCD of four variables in dye removal

Run	X ₁	X ₂	X ₃	X ₄	Removal efficiency (%)	
					Experimental	Model predicted
1	303	4	1.5	60	45.57	45.15
2	313	4	1.5	60	52.97	51.76
3	303	9	1.5	60	46.21	44.34
4	313	9	1.5	60	51.93	50.96
5	303	4	3.5	60	54.00	53.52
6	313	4	3.5	60	63.74	63.19
7	303	9	3.5	60	54.65	54.34
8	313	9	3.5	60	64.65	64.01
9	303	4	1.5	240	54.85	54.41
10	313	4	1.5	240	67.93	68.15
11	303	9	1.5	240	54.65	54.98
12	313	9	1.5	240	68.78	68.72
13	303	4	3.5	240	65.85	66.19
14	313	4	3.5	240	82.13	82.97
15	303	9	3.5	240	67.84	68.39
16	313	9	3.5	240	84.34	85.17
17	298	7	2.5	240	57.43	58.11
18	318	7	2.5	150	81.32	81.59
19	308	2	2.5	150	65.14	65.74
20	308	11	2.5	150	66.43	66.99
21	308	7	0.5	150	45.34	47.16
22	308	7	5	150	73.23	72.68
23	308	7	2.5	15	39.67	43.74
24	308	7	2.5	300	68.00	65.83
25	308	7	2.5	150	64.87	64.66
26	308	7	2.5	150	64.87	64.66
27	308	7	2.5	150	64.87	64.66
28	308	7	2.5	150	64.87	64.66
29	308	7	2.5	150	64.87	64.66
30	308	7	2.5	150	64.87	64.66
31	308	7	2.5	150	64.87	64.66

also decreases with increasing the solute concentration. This indicates that the adsorption capacity is a robust function of temperature. Similar temperature effects on the adsorption of BG dye on bagasse fly ash was also observed by Mane et al. [29] and the increase in sorption capacity with an increase in temperature may be attributed to chemisorptions [30]. The internal pores of adsorbent along with viscosity of dye solution exhibit a sinusoidal effect and have a strong negative influence on the adsorption process.

3.7. Optimization of dye adsorption by RSM

The response surface regression (RSREG) procedure for SAS was employed to fit the second-order polynomial equation for the obtained experimental data, represented as percentage removal efficiency of BG. The models were selected based on the highest order polynomials. The quadratic model was selected as suggested by the employed software. The 2⁴ full factorial experiments were planned to obtain a quadratic model consisting of trials plus a star configuration ($\alpha = \pm 2$) and replicates at the center point. The design of this experiment is given in Table 3, together with the experimental results. The maximum adsorption of BG was found to be >84%. Regression analysis was performed to fit the response function of removal of BG (%). The model was expressed by Eq. (5). From the SAS output of RSREG, the final empirical model in terms of coded factors for adsorption of BG (Y) is given in Eq. (7):

$$Y = 84.74 - 3.46X_1 - 1.65X_2 + 4.56X_3 + 0.07X_4 + 0.15X_1X_3 + 0.16X_2X_3 + 0.01X_3X_4 + 0.05X_1^2 + 0.09X_2^2 - 1.23X_3^2 \tag{6}$$

Based on the developed mathematical model equations, an increase of the BG percentage removal or maximization of the BG dye adsorption onto adsorbent was required. The quadratic model equation was optimized using quadratic programming. The optimum adsorption conditions for a new adsorbent resulted in: temperature 313 K, pH 9, adsorbent dose 3.5 g/L of aqueous dye solution, and contact time 240 min. The model validations have been determined as optimum levels of the process parameters to achieve the maximum adsorption of dye of 85.17%, compared to 84.34%.

From the Student's *t*-test results, it was observed that the coefficient of interaction between contact time and temperature is highly significant at 99.99% confidence level (*P* value=0.00), but negative with a *t*-value of 5.012. However, the interaction between other parameters like temperature and dosage and dosage and time was also highly significant at >95% with *P* value of 0.058 and 0.037, respectively. From the regression analysis, as shown in Table 4, the second-order polynomial model equation was statistically significant and adequate to represent the actual relationship between the removal efficiency on the experimental parameters with a very small *P* value (>99.99%) and satisfactory coefficient of

Table 4
Estimated regression coefficients and Student's *t*-test for BG removal

Term	Coefficient	Standard deviation	<i>t</i>	<i>p</i>	Remarks
Constant	84.74	19.1255	4.430	0.000	–
X ₁	–3.46	0.9027	–3.836	0.001	Significant
X ₂	–1.65	1.3340	–1.235	0.235	–
X ₃	22.81	15.4654	1.475	0.160	–
X ₄	0.07	0.0347	1.942	0.070	Significant
X ₁ ²	0.05	0.0117	4.475	0.000	–
X ₂ ²	0.09	0.0542	1.630	0.123	–
X ₃ ²	–30.81	5.5440	–5.557	0.000	–
X ₄ ²	–0.00	0.0001	–10.291	0.000	–
X ₁ X ₂	0.00	0.0297	0.002	0.998	–
X ₁ X ₃	0.76	0.3731	2.042	0.058	Significant
X ₁ X ₄	0.00	0.0008	5.012	0.000	Significant
X ₂ X ₃	0.81	0.7408	1.099	0.288	–
X ₂ X ₄	0.00	0.0016	0.925	0.368	–
X ₃ X ₄	0.05	0.0207	2.277	0.037	Significant

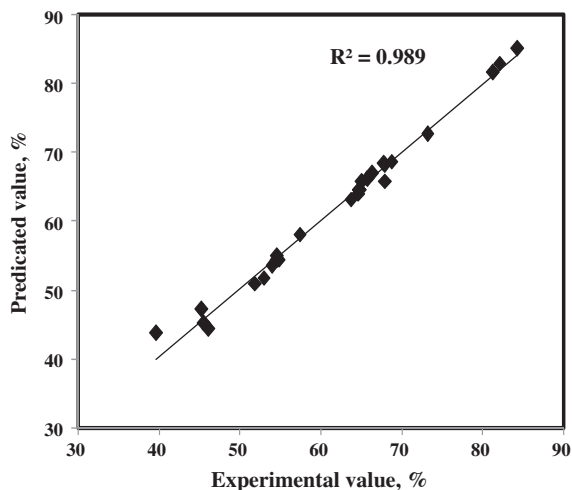


Fig. 8. Experimental values (%) plotted against the predicted values (%) derived from the model of BG dye.

determination ($R^2=0.93$). Furthermore, absolute average deviation (AAD) between the predicted and observed data is highly significant (AAD=1.492). So, R^2 and AAD values for the three models indicate that the model equations are adequate to describe the experimental designs. Verification experiments performed at the predicted conditions derived from the ridge analysis of RSM demonstrated that the experimental values were reasonably close to the predicted values (Table 3), indicating the validity and adequacy of the predicted models. The experimental value versus predicted value displays the real responses data plotted against the predicted responses, which is evidence by Fig. 8. The actual values are the measured response data for a particular run and the predicted values are evaluated from the model and are generated by using the approximating functions. It is also observed that there is a tendency in the linear regression fit, and the model adequately explains the experimental range studied. The fitted regression equation showed a good fit of the model with $S=1.492$, $R^2=98.9\%$, and R^2 (adj) = 98.0%, respectively.

ANOVA of BG removal obtained in this study is presented in Table 5. In general, ANOVA explains any variation in the statistically derived model and significance of the model parameters. The model parameters usually indicated in ANOVA are the main effects, interaction effects, and error terms, and their significance in the model is represented by Fischer "F" and associated P values. The other items in the ANOVA table are degrees of freedom (DF), sum of squares (SS), and mean squares (MS). The MS value of a model term in

the ANOVA table is obtained by dividing SS over DF and its F value is obtained by dividing MS due to the model term by MS due to error [22]. Normally, a larger F and lower P value of a model term in ANOVA indicates good significance of the term over the others. In this study, both models obtained for the two initial concentration ranges were able to explain the experimental results on BG removal accurately with a chance of only <0.1% variation. Fig. 9 shows the resulting response surface and contour plots of the maximum point of response based on the effect time, dosage at temperature of 303K, and pH of 7.

Table 5
ANOVA for BG removal by *C. limetta* peel adsorbent

Factors	DF	SS	MS	F	P
Regression	14	3,351.278	239.3770	107.49	0.000
Linear	4	64.882	16.2205	7.28	0.002
Square	4	324.740	81.1849	36.45	0.000
Interaction	6	81.238	13.5397	6.08	0.002
Residual error	16	35.632	2.2270	–	–

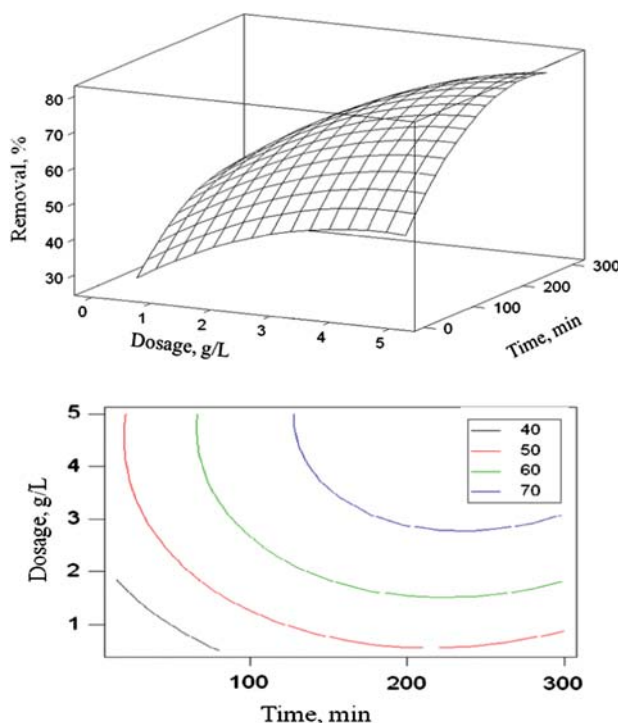


Fig. 9. Response surface and contour plot of BG dye removal (%) by the adsorbent showing interactive effect of time and dosage.

4. Conclusion

Adsorption of BG dye by a low-cost adsorbent prepared from *C. limetta* peel was studied in batch shake flasks. The BG dye percentage removal was found to increase by increasing adsorbent dosage and temperature and decreasing with the initial concentration. Through analysis of the RSREG derived from the models, temperature and contact time took the most significant effect on BG adsorption. The experimental runs were optimized using CCD and the optimized parameters are in good agreement with those obtained in experiments. The ANOVA showed experimental results on BG removal accurately with a chance of only <0.1% variation. RSM showed a better prediction in optimizing the operating parameters in adsorption processes. Overall, the study revealed the potential of the low-cost adsorbent in removing BG dye.

Acknowledgment

The assistance from Department of metallurgical and materials engineering, NIT Tiruchirappalli for SEM imaging is gratefully acknowledged.

References

- [1] B. Acemioglu, Adsorption of Congo red from aqueous solution onto calcium-rich fly ash, *J. Colloid Interface Sci.* 274 (2004) 371–379.
- [2] L. Nicolet, V. Rott, Recirculation of powdered activated carbon for the adsorption of dyes in municipal wastewater treatment plants, *Water Sci. Technol.* 40 (1999) 191–198.
- [3] Y. Al-Degs, M.A.M. Kharaisheh, S.J. Allen, M.N. Ahmad, Effect of carbon surface chemistry on the removal of reactive dyes from textile effluent, *Water Res.* 34 (2000) 927–935.
- [4] A. Gurses, C. Dogar, M. Yalcin, M. Acikyildiz, R. Bayrak, S. Karaca, The adsorption kinetics of the cationic dye, methylene blue, onto clay, *J. Hazard. Mater.* 131 (2006) 217–228.
- [5] M.P. Gupta, P.K. Bhattacharya, Studies on colour removal from bleach plant effluent of a kraft pulp mill, *J. Chem. Technol. Biotechnol.* 35 (1985) 23–32.
- [6] S.S. Baral, S.N. Das, P. Rath, Hexavalent chromium removal from aqueous solution by adsorption on treated sawdust, *Biochem. Eng. J.* 31 (2006) 216–222.
- [7] D. Mohan, K.P. Singh, G. Singh, K. Kumar, Removal of dyes from wastewater using flyash, a low-cost adsorbent, *Ind. Eng. Chem. Res.* 41 (2002) 3688–3695.
- [8] Q. Sun, L. Yang, The adsorption of basic dyes from aqueous solution on modified peat-resin particle, *Water Res.* 37 (2003) 1535–1544.
- [9] M.M. Abd El-Latif, A.M. Ibrahim, Adsorption, kinetic and equilibrium studies on removal of basic dye from aqueous solutions using hydrolyzed oak sawdust, *Desalin. Water Treat.* 6 (2009) 252.
- [10] S. Wang, Y. Boyjoo, A. Choueib, A comparative study of dye removal using fly ash treated by different methods, *Chemosphere* 60 (2005) 1401–1407.
- [11] S. Wang, L. Li, Z.H. Zhu, Solid-state conversion of fly ash to effective adsorbents for Cu removal from wastewater, *J. Hazard. Mater.* 139 (2007) 254–259.
- [12] M. Matheswaran, Kinetic studies and equilibrium isotherm analyses for the adsorption of Methyl Orange by coal fly ash from aqueous solution, *Desal. Wat. Treat.* 29 (2011) 241–251.
- [13] B.H. Hameeda, M.I. El-Khaiary, Malachite green adsorption by rattan sawdust: Isotherm, kinetic and mechanism modeling, *J. Hazard. Mater.* 159 (2008) 574–579.
- [14] S. Wang, H. Wu, L. Li, Z.H. Zhua, Unburned carbon as a low-cost adsorbent for treatment of methylene blue-containing wastewater, *J. Colloid Interface Sci.* 292 (2005) 336–343.
- [15] M. Meilgaard, G.V. Civille, B.T. Carr, Advanced statistical methods, In: *Sensory Evaluation Techniques*, second ed., CRC Press, Boca Raton, FL, 1991, pp 275–304.
- [16] M. Otto, *Chemometrics: Statistics and Computer Applications in Analytical Chemistry*, Wiley-VCH, Chichester, 1999.
- [17] C. Lizama, J. Freer, J. Baeza, H.D. Mansilla, Optimized photodegradation of Reactive Blue 19 on TiO₂ and ZnO suspensions, *Catal. Today* 76(2) (2002) 235–246.
- [18] A. Danion, C. Bordes, J. Disdier, J.V. Gauvrit, C. Guillard, P. Lanteri, Optimization of a single TiO₂-coated optical fiber reactor using experimental design, *J. Photochem. Photobiol., A* 168(3) (2004) 161–167.
- [19] J. Fernandez, J. Kiwi, J. Baeza, J. Freer, C. Lizama, H.D. Mansilla, Orange II photocatalysis on immobilised TiO₂: Effect of the pH and H₂O₂, *Appl. Catal.* 48(3) (2004) 205–211.
- [20] A. Gurses, M. Yalcina, C. Dogar, Electrocoagulation of some reactive dyes: A statistical investigation of some electrochemical variables, *Waste Manage.* 22 (2000) 491–494.
- [21] K. Ravikumar, K. Pakshirajan, T. Swaminathan, K. Balu, Optimization of batch process parameters using response surface methodology for dye removal by a novel adsorbent, *Chem. Eng. J.* 105 (2005) 131–138.
- [22] D.C. Montgomery, *Design and Analysis of Experiments*, third ed., Wiley, New York, NY, 2002, pp 270–569.
- [23] J.F. Fu, Y.Q. Zhao, X.D. Xue, W.D. Li, A.O. Babatunde, Multivariate-parameter optimization of acid blue-7 wastewater treatment by Ti/TiO₂ photoelectrocatalysis via the Box-Behnken design, *Desalination* 243 (2009) 42–51.
- [24] R.Y. Talman, G. Atun, Effects of cationic and anionic surfactants on the adsorption of toluidine blue onto fly ash, *Colloids Surf., A* 281 (2006) 15–22.
- [25] R.H. Myers, D.C. Montgomery, *Response Surface Methodology: Process and Product Optimization Using Designed Experiments*, second ed., Wiley, New York, NY, 2002.
- [26] G. Box, W.G. Hunter, *Statistics for Experimenters: An Introduction to Design, Data Analysis, and Model Building*, Wiley, New York, NY, 1978.
- [27] Ru-Ling Tseng, Szu-Kung Tseng, Wu Feng-Chin, Preparation of high surface area carbons from Corn cob with KOH etching plus CO₂ gasification for the adsorption of dyes and phenols from water, *Colloids Surf., A* 279 (2006) 69–78.
- [28] D.M. Ruthven, *Principles of Adsorption and Desorption Processes*, Wiley, New York, NY, 1984.
- [29] V.S. Mane, I.D. Mall, V.C. Srivastava, Use of bagasse fly ash as an adsorbent for the removal of brilliant green dye from aqueous solution, *Dyes Pigment.* 73 (2007) 269–278.
- [30] V.C. Srivastava, M.M. Swamy, I.D. Mall, B. Prasad, I.M. Mishra, Adsorptive removal of phenol by bagasse fly ash and activated carbon: Equilibrium, kinetics and thermodynamics, *Colloid Surf., A* 272 (2006) 89–104.